Solar Physics (2006) 235: 17–29
DOI: 10.1007/s11207-006-0041-5

CARRINGTON COORDINATES AND SOLAR MAPS

ROGER K. ULRICH and JOHN E. BOYDEN
Department of Physics and Astronomy, UCLA, 430 Portola Plaza, Los Angeles, CA 90095-1547, USA
(e-mail: ulrich@astro.ucla.edu)

(Received 8 August 2005; accepted 30 December 2005)

Abstract. Solar synoptic charts are normally displayed using Carrington Coordinates with each Carrington rotation being centered at a Carrington longitude of 180° and with a full 360° of solar surface properties included. For the case of reproducing solar magnetic fields in the corona and heliosphere, these maps are wrapped onto the solar surface to provide the boundary conditions for a solution to a set of modeling equations such as the potential field theory equations. Due to differential rotation, the full solar surface cannot be reproduced in this fashion since different parts of the solar surface are observed at different times. We describe here the proper technique for combining observations of the solar magnetic or velocity fields made at different times into a representation of the whole solar surface at a particular specified time that we refer to as a "snapshot heliographic map".

1. Introduction

The display of properties of the solar surface in terms of time, location, and strength depends on the definition of a coordinate system for the Sun. Since the Sun is gaseous and has no permanent demarcation points to use as a reference, the convention established by Carrington (1863) has been followed based on a fixed rotation rate and an arbitrary zero point. For any observation of a feature or physical quantity on the apparent solar disk, standard methods of spherical astronomy, such as described by Smart (1962), can be used to convert the position of measurement expressed as an angular offset relative to fixed points on the apparent solar disk (typically x, y angular distances relative to the disk center based on the solar axis of rotation as the y axis) to a heliographic latitude and longitude with the latter taken relative to the zero point defined by Carrington. The detailed methods of converting solar observations into modern coordinate systems have been described recently by Thompson (2006). When a number of observations from many days are combined and plotted relative to the Carrington longitude and latitude, the resulting figure is called a "synoptic chart", and Carrington (1863) was the first to produce such charts. The rotation rate was chosen by Carrington to track the apparent movements of sunspots across the solar disk. Carrington also recognized that many features move relative to these coordinates, and he used what is now called a stackplot to illustrate these displacements.

Full-Sun magnetic maps can be used either to represent conditions on the solar surface at a particular point of time in the past in the most satisfactory manner or to project conditions into portions of the solar surface that are not observed. For the first purpose, it has been common to create synoptic charts based on the best observed portions of the solar surface near the Sun's central meridian, and this is the format usually encountered. For the projection into portions of space and time where observations are not available, physics-based, flux-transport models have been used by a number of workers (Devore *et al.*, 1985; Worden and Harvey, 2000; Schrijver, 2001; McCloughan and Durrant, 2002; Durrant and McCloughan, 2004) to make predictions of magnetic-field strength. These predictive treatments have been careful to treat the solar surface in coordinates at a particular instant in time through a remapping process. We are concerned in the present paper with the task of representing observed properties of the Sun in the most reliable manner and in the preparation and interpretation of synoptic charts. Such charts have been used by for example Worden and Harvey (2000) as input to the physics-based model and by Arge and Pizzo (2000) in the computation of properties of the solar wind. We provide in the present paper methods of treating the variables used in standard synoptic charts in a manner that properly accounts for the distorting effects of differential rotation.

Solar longitude is an angle giving position on the solar surface at a particular moment of time. A traditional synoptic chart extracts properties of the solar surface that are near the central meridian at the time of observation and includes only a limited range of central meridian angle. For central meridian angles larger than about $\pm 20^{\circ}$, differential rotation causes features to change their heliographic longitude as a function of observation time so that averages over multiple observations are smeared. Synoptic charts are most commonly prepared using Carrington's rotation rate to define longitude. The smearing we correct comes from the difference between a feature's rotation rate at a particular latitude and the Carrington rate. Generally the feature rates are smaller than the Carrington rate because the higher latitudes rotate much more slowly than the near-equator regions. Some features such as magnetic patterns have a rotation rate greater than the Carrington rate near the equator. The methods described here apply to all forms of differential rotation rate although the figures have been prepared using the magnetic feature rate. If we had used the rotation rate appropriate to the Doppler-shift velocities, all portions of the solar surface would rotate more slowly than the Carrington rate.

The Mt. Wilson group has corrected each observation for the effect of differential rotation prior to summing (Ulrich *et al.*, 2002; Ulrich and Boyden, 2005). In order to distinguish these synoptic charts from traditional synoptic charts we use the term "Differential Rotation Corrected" synoptic charts or "DRC" charts for the resulting representations. We have also reversed the abscissa and plotted multiple DRC charts next to each other to create what we term a supersynoptic chart. In the supersynoptic chart format, the abscissa is in fact the time of central meridian crossing for each point. This paper gives the details of the transformations needed to carry out this

differential-rotation correction in order to produce one of two types of synoptic map: (1) a DRC synoptic chart in which the abscissa is not a longitude angle and (2) a "Snapshot Map" which is a DRC heliographic map in which the abscissa is a longitude angle at a specific time.

Our treatment is based on the correspondence between Carrington longitude and time. The central meridian (CM) crossing time of Carrington longitude 0° for Carrington rotation zero defines a starting point for a time–like variable which then progresses forward at a rate of one unit per synodic Carrington rotation period. This definition is presented in more detail in the next section of the paper. The Carrington Rotation Number (N) is the integer number of Carrington rotations from this starting time. We can denote the time that a point crosses the CM as the real number of Carrington units including the fractional part of the rotation. The convention of having the longitude increase from East to West while the western parts of the solar surface cross the CM before the eastern parts means that within each Carrington rotation, the heliographic longitude of the CM decreases with time. Consequently, the fractional part of the rotation appropriate to Carrington longitude L (in degrees) crossing the CM is $1 - (L/360^\circ)$ instead of $L/360^\circ$. To make it explicit that this longitude-like time of CM crossing measured in Carrington rotation units is not an integer, we term this variable the "Carrington time" of the point and use the symbol τ^N. The superscript N denotes the Carrington rotation number on which the point crosses the CM and is included for reasons discussed below.

We illustrate with a specific example of the calculations needed to carry out this differential rotation correction. Figure 1 shows an arbitrary sample observation of the solar surface at a time when the CM is at Carrington longitude 140° and a sample point is observed at **a**. We have picked point **a** so that it will cross the CM three-quarters of a Carrington rotation after the most recent CM crossing of Carrington longitude 0°. At the time of this observation, the point is not at Carrington longitude 90° because it rotates more slowly and is at a negative Central Meridian Angle (CMA) closer to zero as shown. If we replace the point's observed heliographic longitude by its heliographic longitude at the time it crosses the CM, we will have a longitude-like variable which will remain constant provided we have adopted the proper rotation rate for the latitude in question. The shift in the effective longitude brings the point from **a** to **b** in Figure 1. Notice that for this observation, the time of CM crossing is $(140 - 90)/360$ Carrington rotations later than the time of observation; *i.e.* the CMA offset is negative while the time offset is positive due to the conventional definition of heliographic longitudes. This example illustrates the tranformations we need to carry out in general in order to correct for differential rotation.

Each magnetic feature on the solar surface has a unique CM crossing time τ^N during Carrington rotation N. At higher latitudes, the time interval between successive CM crossings by a magnetic feature is greater than the Carrington rotation period; *i.e.* the Carrington time interval between successive CM crossings is greater than unity. Because the Carrington time advances one unit per Carrington rotation,

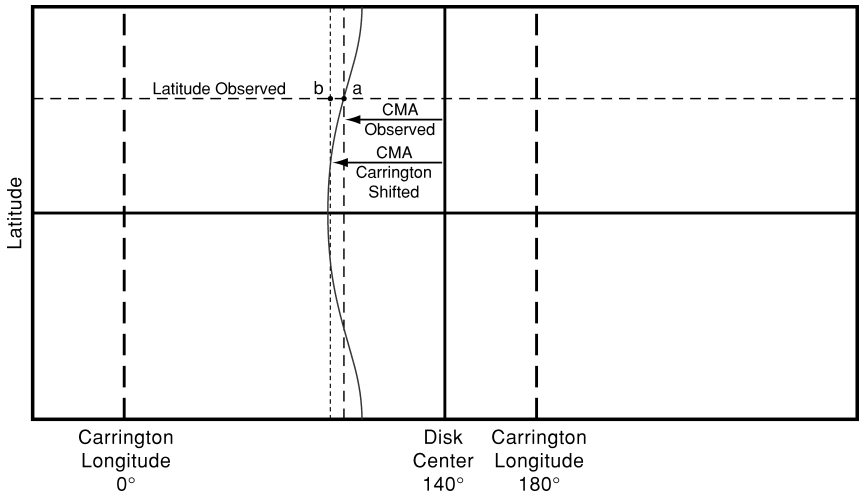

Figure 1. The smearing effect of differential rotation and the shift needed to correct for the effect by shifting the position of the observed point. The heavy outer rectangle defines the edges of the map of the full solar surface at the time of observation based on the solar axis of rotation. The heavy solid lines within the rectangle give the solar equator and central meridian. The heavy dashed lines show the location of the Carrington longitude 0° and 180° points for this example. A typical point is observed at position **a** with a central meridian angle CMA. Based on its latitude, we can determine the time required to reach the central meridian. The locus of points requiring this length of time is shown as the light solid line passing through **a**. We shift the point to location **b** so that it would take that same interval of time if it were rotating with the Carrington rate. Points from separate observations will have a different central meridian angles but they all have the same central meridian crossing time and are shifted by an angle calculated according to the above geometry, they will all represent the same solar surface feature and will not be smeared.

while magnetic features have a rotation rate different from the Carrington rate, the Carrington time for a feature on successive CM crossings does not advance by unity. For example at a latitude near 60°, the rotation rate is about 20% slower than the Carrington value so that a feature crossing the CM at a Carrington time of, say, 1950.5 will cross the CM after the Carrington time advances by 1.25 at a Carrington time of 1951.75. Successive transits of the CM are not separated by unity in Carrington units except at that latitude where the rotation rate equals the Carrington value. This is why high latitude features drift relative to the Carrington longitudes when plotted using a stackplot format. This property of a tracked feature is expressed formally by the statement: $\tau^{N\pm1} \neq \tau^N \pm 1$. Clearly, we need to specify N in order to fully define the Carrington time of the feature. Pairs of points at different latitude but identical τ^N are aligned in a North/South configuration when they cross the CM on Carrington rotation N. By using τ^N as the longitude-like variable to define position on the solar surface, we avoid the smearing effect and can include observations from more than one Carrington rotation so that we can carry out time-series analyses restricted only by the lifetimes of features.

It is possible to treat the Carrington time as a combination of Carrington rotation number (N) and a longitude offset angle. The resulting chart has a form identical to that of a traditional synoptic chart. Although the abscissa has units of longitude angle, it is not a true longitude in that pairs of points along lines of constant latitude are not separated by this angular difference except on a latitude which rotates at the Carrington rate. We call a plot of magnetic fields made in this way a DRC synoptic chart and refer to the longitude calculated this way as a Carrington-time equivalent longitude. It is important to remember that a DRC synoptic chart never represents the whole solar surface at a single time; time and space are intermingled in the abscissa values. If a chart of the surface using true longitudes is required, it is necessary to select a mapping time and then distort the synoptic chart in a manner that reverses the original differential rotation correction and yields the longitude of each point. We call these redistorted plots "snapshot heliograph maps". The following section gives the explicit transformations for both summing quantities into a DRC synoptic chart and for recovering snapshot heliographic maps from the charts.

One of our objectives is to apply time series analysis methods to the prediction and interpolation of solar properties for times when a point is not on the visible portion of the solar surface. As a first step in this direction, the final section provides a simple extension of the methods introduced by Shrauner and Scherrer (1994) for treating the effect of solar rotation on the projections of vector quantities onto the line of sight.

2. Map Transformations

2.1. The approach

The correction for the effects of differential rotation involves the following steps:

- Observation: Shift each observed point in space to a position in the final chart where it remains fixed according to some differential rotation law.
- Summing: Carry out an appropriate time series analysis to derive quantities of interest such as for example the correlation of magnetic field with viewing angle or a dense-pack ring diagram analysis with helioseismic techniques (Haber *et al.*, 2002; Komm *et al.*, 2004). These results are presented in the DRC synoptic chart format.
- Mapping: Distort the DRC chart back into a snapshot heliographic map. This step is essentially the inverse of the first step.

We start the discussion of an implementation of the above steps by casting the equations in terms of the Carrington time. As noted above, the Carrington longitude has the undesirable properties of running backwards relative to time modulo 360° while the Carrington rotation number moves forward in time. Consequently,

a time-like variable cannot be composed out of the Carrington longitude and the Carrington rotation number by adding $L/360$ to N. This property of the Carrington longitude makes it difficult to present simple formulae for the treatment of differential rotation. The use of the Carrington time as an intermediary simplifies the exposition.

2.2. CARRINGTON TIME

As a convention for this paper we measure time in Carrington units which are the real number of solar rotations at a fixed synodic rate of 27.2753 days per rotation beginning at a zero time defined by Carrington (1863) for which Carrington rotation 1 commenced November 9, 1853. This convention applies to both times of observation indicated by $t_{\rm obs}$ as well as the definition of the longitude-like Carrington time τ^N. Our methods can be applied to observations spanning multiple Carrington rotations but in such applications it is important to remember that for most latitudes $\tau^{N\pm1} \neq \tau^N \pm 1$. Charts and maps prepared with our methods must always specify the Carrington rotation number to which they apply; hence, we include N in the definition of τ^N. When a point is on the CM, the time of observation, $t_{\rm obs}$ is equal to τ^N. Since τ^N is a real number, the integer Carrington rotation number must obey $N = \lfloor \tau^N \rfloor$ where the lower bracket symbols denote the floor function which returns the largest integer N not greater than τ^N. Although, we mostly use values of τ^N where $N = \lfloor \tau^N \rfloor$, this is not a requirement and for some applications of time series analysis, it is necessary to include observations which violate this equality. In that case it is important to treat these observations according to the formalism below, since positions on successive rotations do not line up at all latitudes.

The relationship between the CM longitude, L_0^N, (in degrees) and the Carrington time, τ^N, is[1]

$$L_0^N = 360^\circ(N + 1 - \tau^N)\,. \tag{1}$$

Using standard geometric relationships we can calculate the longitude of each observed point $L_{\rm obs}^{N'}$ where N' may differ from N if the CM is on a different Carrington rotation. The longitude increases in the direction of rotation and the time of CM crossing becomes earlier than the time of observation as the longitude

[1]The CM is displaced from this location by a small amount due to the eccentricity of the Earth's orbit. An easy way to understand this offset is to imagine solarians (dwellers on the surface of the Sun) observing the Earth from an "observatory" on the Sun rotating at a fixed Carrington rate. Synodic Carrington time would be local mean time kept by the solarians if they adopted transits of the Earth as their local midnight. A time lapse photograph of the Earth taken by the solarians with a camera pointed in a constant direction relative to their observatory co-ordinates and with exposures made at a fixed time on the basis of their local mean time throughout the Earth's year would produce an analemma. We include this offset in calculating the actual location of the CM but do not include changes in this offset as part of the differential rotation correction. Formulae in the text omit this offset for clarity.

becomes more positive. The angular separation between the observed point and the central meridian $\delta L_{\rm obs}$ is then given by:

$$\delta L_{\rm obs} = L_{\rm obs}^{N'} - L_0^N - 360^\circ(N' - N)\,. \tag{2}$$

2.3. DIFFERENTIAL ROTATION CORRECTION

In order to treat differential rotation, we note that at latitude B the time offset in seconds relative to the time of CM crossing is $-\delta L_{\rm obs}/\,\Omega(B)$ where longitude is measured in radians, Ω is in radians per second, and a positive time offset applies to a CM crossing prior to the time of observation. This offset is converted to a fractional Carrington rotation through multiplication with the Carrington rotation rate. The synodic rotation curve we use gives magnetic stackplots with the minimum drift in time:

$$\Omega(B) = 2.730 - 0.4100[\sin^2(B) + 1.0216\sin^4(B)]\mu\text{rad/s}\,. \tag{3}$$

This rate is faster than the widely-used Snodgrass (1983) and Snodgrass and Ulrich (1990) rates which are based respectively on cross-correlations of Doppler velocities and magnetic features over intervals of one to three days. Our rate tracks the longer-lived features which are of interest over periods of one or more solar rotations. The Carrington time for the point for each observation is the Carrington time at the CM of the observation (*i.e.* the time of the observation in Carrington units) corrected by the time displacement of the point from the CM crossing measured in Carrington rotations. For completeness, we note that the synodic Carrington rotation rate $\Omega_{\rm Carr}$ is 2.66622375 μrad/s (the precision given here reflects the conversion from sidereal to synodic units; the Carrington rate is typically stated in sidereal units whereas our rate in Equation (3) has been determined in synodic units). If we represent the longitude in degrees we can express the Carrington time referenced to rotation N for this point when it is observed as:

$$\tau_{\rm obs}^N = t_{\rm obs} - \frac{\delta L_{\rm obs}\,\Omega_{\rm Carr}}{360^\circ\,\Omega(B)}\,. \tag{4}$$

Figure 2 illustrates this transformation. The blue grid represents the angular position of points on the solar surface. For the sake of illustration we have shown a sample point as the dark red circle. Lines of constant Carrington time are shown in black.

Time series analysis can be carried out by incorporating data from a number of observations each having a different $t_{\rm obs}$. The resulting parameters describing the solar surface apply to a grid of latitudes and Carrington times: B, τ^N. We can apply the equivalent of Equation (1) to obtain a longitude-like quantity $\tilde{L}$ which would be the Carrington longitude if the Sun rotated rigidly at the Carrington rate:

$$\tilde{L}^N = 360^\circ(N + 1 - \tau^N) \tag{5}$$

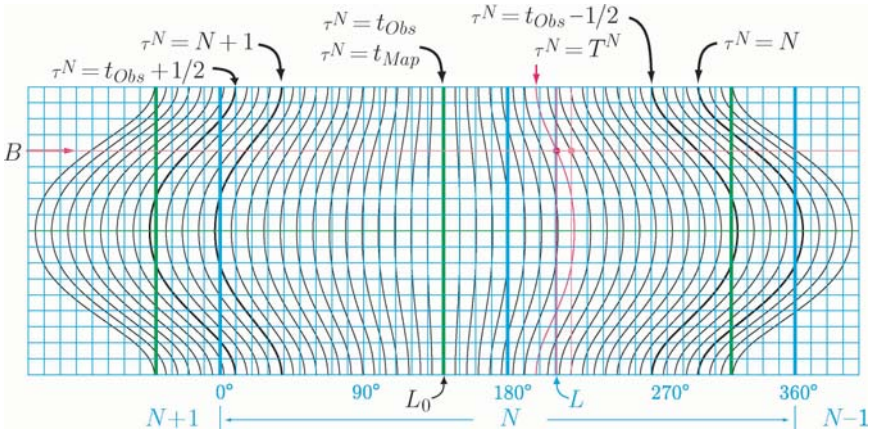

Figure 2. The observed heliographic longitudes as the grid of blue lines and the Carrington times as the grid of black lines. It can be applied at the time of each observation in which case the central meridian is labeled as $\tau^N = t_{\rm obs}$ and at the time of mapping a synoptic chart back to heliographic coordinates in which case the central meridian line is labeled as $\tau^N = t_{\rm map}$. The central meridian is shown as the heavy green line near the map center. The boundaries of the portion of the map representing the entire solar surface are also shown as a pair of heavy green lines a distance of $\pm 180^\circ$ from the central meridian. This figure is intentionally not centered on a Carrington longitude of 180° so that the edges of the surface do not correspond to 0° to 360°. The nearest Carrington rotation boundaries and center line are shown as the heavy blue lines. Note also the convention of plotting the time as increasing from right to left. This is done so that the longitude projected onto the sky increases from left to right when the images are plotted as seen. A particular point on the image is shown as the dark red circle along with dark red lines representing the appropriate latitude and longitude for the point. The observed Carrington longitude for the point is marked on the bottom of the figure with the blue L. The Carrington time of the point is indicated on the top of the figure as the black T^N. After the differential-rotation correction, the point is shifted to the Carrington time equivalent longitude indicated by the light red circle.

with the value of N being given as before from $N = \lfloor \tau^N \rfloor$. Following the definition in the preceeding section, we refer to $\tilde{L}^N$ as the Carrington-time equivalent longitude. Synoptic charts of the derived quantity (such as a simple average) can then be plotted as a function of $\tilde{L}$ and appear as a normal synoptic chart but to distinguish these from the traditional synoptic charts, we refer to them as the "differential rotation corrected synoptic charts" (DRC charts). The DRC chart has points shifted further from the CM since they rotate more slowly at higher latitudes and the progression of points across the DRC chart is uniform at the Carrington rate. However, $\tilde{L}$ cannot be used to represent the longitude of a point at any specified time since the values of L that go into the average are different for each observation.

The final step in the process is to select a mapping time ($t_{\rm map}$), and carry out the reverse distortion so that the position of features on the solar surface can be properly represented. The Carrington longitude of the CM is given by:

$$L_0^N = 360^\circ (N + 1 - t_{\rm map}) \, . \tag{6}$$

with the value of N being given by the floor function applied to $t_{\rm map}$. The longitude of any point on the solar surface can be considered as:

$$L_{\rm map} = L_0^N + \delta L_{\rm map} \, . \tag{7}$$

We then consider all values of $\delta L_{\rm map}$ between -180° and 180° and locate the appropriate positions on the DRC charts that correspond to these points. We are not required in this calculation to constrain $L_{\rm map}$ to the range 0° to 360° but for a final display will need to label the points with values within this range using the modulo function. A rotation number similar to a Carrington rotation number could be used to label the portions of the plot altered by the modulo function following the layout illustrated in Figure 2. With $\delta L_{\rm map}$ in degrees, the Carrington time for each point on the snapshot map is found from:

$$\tau_{\rm map}^N = t_{\rm map} - \frac{\delta L_{\rm map} \; \Omega_{\rm Carr}}{360^\circ \; \Omega(B)} \, . \tag{8}$$

As before, the synoptic map longitude corresponding to this Carrington time can be found and the value of the desired quantity calculated by interpolation from the stored data. When displayed in this format, the abscissa is a true longitude and not a Carrington-time equivalent longitude.

2.4. Sample Reductions

We illustrate the three forms of charts and maps in Figure 3, which utilize all available Mt. Wilson observations for Carrington rotation 1952. For the traditional synoptic chart and the DRC synoptic chart, 464 observations are included. For the snapshot heliographic map, 513 observations are included. The number is larger for the snapshot map because points on the edge come from a larger time interval. Note that structure is much more visible in the lower two maps than in the traditional case. This is true even at high latitude where features usually do not appear. The snapshot map retains the visible structure but shows that the zones of dominant polarity become distorted at the edges. Evidently, the larger scale structure rotates more like the Carrington rate in contrast with the smaller scale features which follow the differential rotation law found with smaller scale magnetic/Doppler structures and the differential rotation law found directly from the Doppler shift velocities.

3. Rotation, Vectors and Time Dependence

We illustrate the use of the differential-rotation-correction approach by showing its application to the study of magnetic field vector components. The formulae here represent a simple extension of the method of Shrauner and Scherrer (1994) and are a minimal way to include a time-series analysis into the representation of solar magnetic field evolution. Solar rotation causes a stationary vector to have a variable

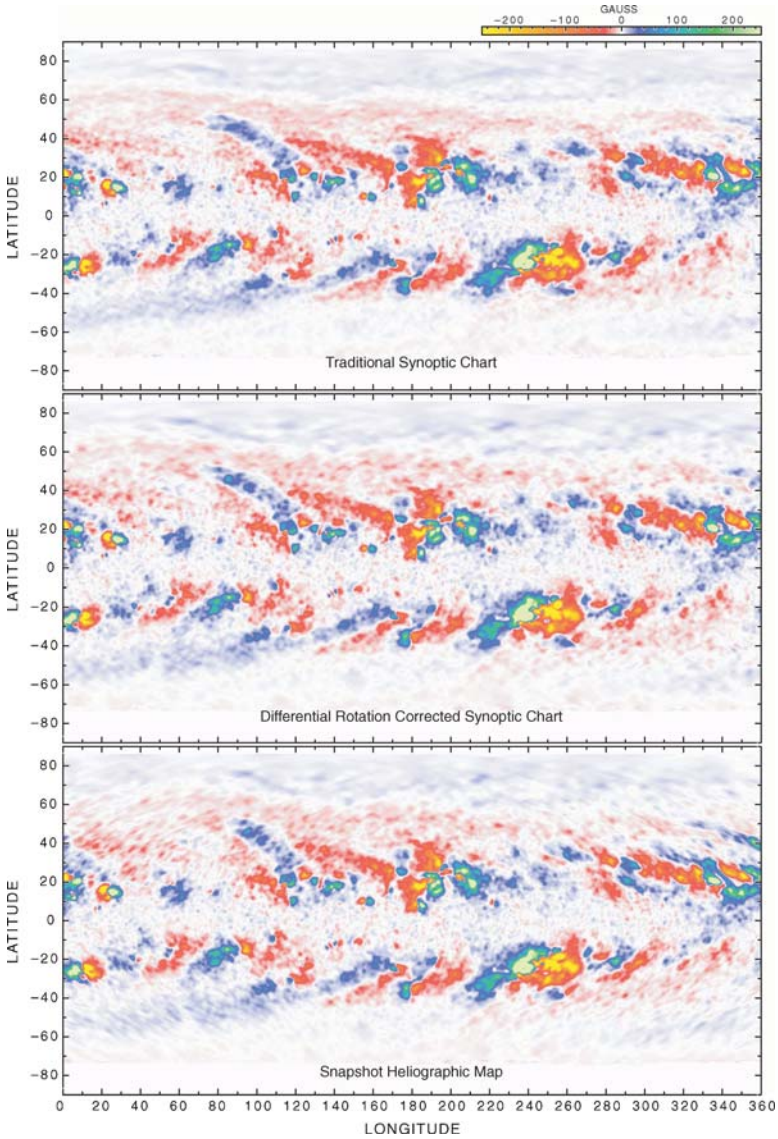

Figure 3. The three forms of synoptic chart discussed in the text. The top figure is a traditional synoptic chart where each observation is added to the Carrington longitude appropriate for its time of observation. We have included all available observations for each point. The second figure carries out the differential rotation correction and plots the points according to their Carrington-time-equivalent longitude. The bottom figure gives the snapshot map for the Carrington time of 1952.5 and so is centered on Carrington rotation 1952. This restriction is done to allow easy comparison to the traditional map on top which follows the convention of restricting the plot to just those longitudes that fall on CR 1952. Although the abscissae for the three plots are all indicated as longitude, they are in fact each different. The top abscissa is the Carrington longitude, the center abscissa is the Carrington-time-equivalent longitude, and the bottom abscissa is the heliographic longitude at the Carrington time 1952.5.

line-of-sight projection. This permits us to resolve the vector magnetic field into two components: one called the zonal magnetic field that is perpendicular to the axis of rotation and the other called the meridional magnetic field that is projected onto the plane of the local longitude. Figures illustrating this decomposition have been given previously (Ulrich *et al.*, 2002; Ulrich and Boyden, 2005). The zonal magnetic field is in an East–West direction while the meridional component is made up of a part that is radial and another that is parallel to the solar surface and in a North–South direction. The method we use cannot distinguish between the two parts of the meridional field. By using more than a single rotation, we can also take account of some time dependence. For each latitude (B) and Carrington time (τ^N) we combine data from observations taken at times t_i and use these to find the magnetic field components at time $t_0 = \tau^N$. The time dependence is then found as a function of the time difference:

$$\Delta t_i = t_i - t_0 \, . \tag{9}$$

For observation i we use the observed CMA δL_i to resolve the slowly varying part of the Sun's magnetic field (B) into meridional and zonal (B_m and B_z) components by representing the line-of-sight component of the magnetic field B_{si} for each observation i as:

$$\mathsf{B}_{si} = \cos(\delta L_i)\mathsf{B}_m + \sin(\delta L_i)\mathsf{B}_z + \Delta t_i \cos(\delta L_i)\dot{\mathsf{B}}_m + \Delta t_i \sin(\delta L_i)\dot{\mathsf{B}}_z \, . \tag{10}$$

We may define weighted sums as follows:

$$sb = \sum_i \sin(\delta L_i)\mathsf{B}_{si} = sc\,\mathsf{B}_m + ss\,\mathsf{B}_z + sct\,\dot{\mathsf{B}}_m + sst\,\dot{\mathsf{B}}_z \tag{11}$$

$$cb = \sum_i \cos(\delta L_i)\mathsf{B}_{si} = cc\,\mathsf{B}_m + sc\,\mathsf{B}_z + cct\,\dot{\mathsf{B}}_m + sct\,\dot{\mathsf{B}}_z \tag{12}$$

$$sbt = \sum_i \Delta t_i \, \sin(\delta L_i)\mathsf{B}_{si} = sct\,\mathsf{B}_m + sst\,\mathsf{B}_z + sctt\,\dot{\mathsf{B}}_m + sstt\,\dot{\mathsf{B}}_z \tag{13}$$

$$cbt = \sum_i \Delta t_i \, \cos(\delta L_i)\mathsf{B}_{si} = cct\,\mathsf{B}_m + sct\,\mathsf{B}_z + cctt\,\dot{\mathsf{B}}_m + sctt\,\dot{\mathsf{B}}_z \tag{14}$$

where

$$\begin{aligned} ss &= \sum_i \sin^2(\delta L_i), \quad sst = \sum_i \Delta t_i \, \sin^2(\delta L_i), \\ sstt &= \sum_i \Delta t_i^2 \, \sin^2(\delta L_i) \\ sc &= \sum_i \sin(\delta L_i)\cos(\delta L_i), \quad sct = \sum_i \Delta t_i \, \sin(\delta L_i)\cos(\delta L_i), \end{aligned} \tag{15}$$

$$sctt = \sum_i \Delta t_i^2 \, \sin(\delta L_i) \cos(\delta L_i) \tag{16}$$

$$cc = \sum_i \cos^2(\delta L_i), \quad cct = \sum_i \Delta t_i \, \cos^2(\delta L_i),$$

$$cctt = \sum_i \Delta t_i^2 \, \cos^2(\delta L_i) \, . \tag{17}$$

In terms of these definitions, we may determine the average zonal and meridional fields by solving the system of Equations (11) to (14). The values for B_m and B_z at the time $t_0 = \tau^N$ have $\Delta t = 0$ so B_m and B_z are independent of $\dot{\mathsf{B}}_m$ and $\dot{\mathsf{B}}_z$. Surface maps of the magnetic field can then be provided using the snapshot reconstruction. Use of a different mapping time (t_0), will produce a different result for the magnetic fields. Field projections using the method of Shrauner and Scherrer (1994) treat the underlying magnetic field as static so that the resulting maps at different times change only because of the varying distortion. By including a minimal representation of the time dependence using the above formulae, the effects of both time variability and variable distortion are present in a series of such snapshot maps.

4. Conclusion

We have defined a variable we term the "Carrington time" and recommend its usage in the context of synoptic charts of solar features. This quantity can either be used in time units or in equivalent angular units. In the latter case, it is desirable to use an alternate symbol or clarify in some manner that the coordinate is not a true longitude. We hope that the use of such labeling will help prevent confusion as to the nature of quantities plotted in synoptic charts. When applying solar data as boundary conditions or input to models, the quantities used should always be taken from a snapshot or instantaneous chart of the variable and not from a synoptic chart. When a synoptic chart is prepared from multiple observations, smearing of features can be reduced by differential rotation correction; and if this method is used, it is important to make explicit which rotation law has been applied.

Acknowledgements

We would like to thank the anonymous referee for suggesting we include Figures 1 and 3. We also thank Jack Harvey and Luca Bertello for reading drafts of this paper and providing helpful comments. Observations and synoptic map preparations based on data from the 150-foot solar tower telescope on Mt. Wilson have been supported at UCLA for the past 19 years by a variety of grants from NASA,

NSF and ONR. Support for the program is currently provided by the NSF through grants ATM-0236682 and ATM-0517729.

References

Arge, C.N. and Pizzo, V.J.: 2000, *J. Geophys. Res.* **105**, 10465.
Carrington, R.C.: 1863, *Observations of Spots on the Sun,* London: Williams and Norgate.
Devore, C.R., Sheeley, N.R., Boris, J.P., Young, T.R., and Harvey, K.L.: 1985, *Solar Phys.* **102**, 41.
Durrant, C.J. and McCloughan, J.: 2004, *Solar Phys.* **219**, 55.
Haber, D.A., Hindman, B.W., Toomre, J., Bogart, R.S., Larsen, R.M., and Hill, F.: 2002, *Astrophys. J.* **570**, 855.
Komm, R., Corbard, T., Durney, B.R., González Hernández, I., Hill, F., Howe, R., and Toner, C.: 2004, *Astrophys. J.* **605**, 554.
McCloughan, J. and Durrant, C.J.: 2002, *Solar Phys.* **211**, 53.
Schrijver, C.J.: 2001, *Astrophys. J.* **547**, 475.
Shrauner, J.A. and Scherrer, P.H.: 1994, *Solar Phys.* **153**, 131.
Smart, W.M.: 1962, *Text-Book on Spherical Astronomy*, Cambridge: Cambridge University Press.
Snodgrass, H.B.: 1983, *Astrophys. J.* **270**, 288.
Snodgrass, H.B. and Ulrich, R.K.: 1990, *Astrophys. J.* **351**, 309.
Thompson, W.T.: 2006, *Astron. Astrophys.* In press.
Ulrich, R.K. and Boyden, J.E.: 2005, *Astrophys. J.* **620**, L123.
Ulrich, R.K., Evans, S., Boyden, J.E., and Webster, L.: 2002, *Astrophys. J. Suppl.* **139**, 259.
Worden, J. and Harvey, J.: 2000, *Solar Phys.* **195**, 247.